Photocatalytic degradation of E. coli bacteria using TiO_2/SiO_2 nanoparticles with photodeposited platinum

Z. Ahmadi [1], Sh. Afshar [1]*, L. Vafaee [1], A. Salehi [2]
1. College of Chemistry, Iran University of Science and Technology, Narmak, Tehran, 16844, I. R. Iran
2. Agricultural Department, Saveh Azad University, Saveh, I. R. Iran
(*)Corresponding author: sh_afshar@iust.ac.ir
(Received; 10 Sep 2008 and Accepted; 20 Dec 2008)

Abstract
In this work, TiO_2/SiO_2 (pure anatase), and TiO_2/SiO_2 (anatase/rutile) nano-photocatalysts are prepared by using sol-gel method and control of acidity. The particles size is calculated using Scheerer s equation and is estimated to be around 7-15 nm. In order to improve the photocatalytic activity of TiO_2/SiO_2 ,1% (wt) platinum particles are loaded on both catalysts using photoreductive method. SEM images show that doping of Pt particles is not homogenous. FT-IR, BET and UV-Vis Reflectance are used to characterize the structures and properties of photocatalysts. The photocatalytic activities of these catalysts are investigated by their bactericidal activities on E. coli bacteria. 100% destruction of E. coli bacteria has occurred under UV light illumination after 5, 15, 20 and 60 min using Pt-TiO_2/SiO_2 (pure anatase), TiO_2/SiO_2 (pure anatase), Pt-TiO_2/SiO_2 (anatase/rutile) and TiO_2/SiO_2 (anatase/rutile) photocatalyst, respectively. The effect of doping Pt is remarkable and rate of destruction using Pt doped catalysts (both catalysts) is three times faster than that of TiO_2/SiO_2 catalysts.
Keywords: *Photocatalysis; E. coli; Sol-gel; TiO_2/SiO_2; Platinum*

1. INTRODUCTION

TiO_2 is the most popular semiconductor used in photocatalytic processes and serious attention has been focused on the photocatalytic performance of TiO_2, due to its good environmental stability, for the purification of contaminated air or water [1,2]. also, different reports have described photokilling of bacteria [3-5], viruses [6] and tumor cells [7] by photocatalytic treatment of water. Generally, TiO_2 photocatalysts generate strong oxidizing power under illumination of UV light with wavelength less than 385 nm by producing holes (h^+) and hydroxyl radicals ($OH^\bullet$) generated in the valence band, and electrons and superoxide ions (O_2^-) generated in the conduction band [8]. Various damages to living organisms are caused by the reactive oxygen species (ROS) generated by TiO_2 photocatalytic reactions. In 1985 Matsunaga and coworkers reported the microbicidal effect of the TiO_2 photocatalysts reactions for the first time [9]. Since then, research work on TiO_2 photocatalytic killing has been intensively conducted on a wide spectrum of organisms includes viruses, bacteria, fungi, algae, and cancer cells. A review of this research has been published by Blake et al [10].

As mentioned above, TiO_2 is the choice of being the best photocatalyst. But, it still is faced to some drawbacks to be the best. Low surface area, especially for industrial catalysts like P-25 (with surface area about 50 m^2/g) [11], and charge combination are the most important faults [12]. These two factors decrease the efficiency of photocatalysts. Therefore, numerous efforts have been carried out to overcome these difficulties. One

way is adding second metal oxide like silica to the TiO_2 [13] to increase the surface area. Second way is adding some metal particle to increase the charge separation. This modification can enhance the photocatalytic activity. The dominant parameters include the nature, the concentration of dopant, and the thermal treatment of the material [12]. Brezova et al. [12] reported the presence of metals such as Li^+, Zn^{2+}, Cd^{2+}, Pt^0, Ce^{3+}, Mn^{2+}, Al^{3+}, and Fe^{2+}, may significantly change the photoactivity of TiO_2. Addition of noble metals such as Pt on TiO_2 may provide two types of enhancement effects on pollutant degradation; one is the photocatalytic activity attributable to increase the charge separation efficiency and the other is thermocatalytic activity attributable to surface of nanoparticle metals. The increase in charge separation efficiency will enhance the formation of active oxygen species which improves the degradation rate. The thermocatalytic activity may enhance the dark reactions in pollutant degradation and the active species formed by UV absorption would be efficiently utilized for the light reaction. This scheme will be effective on the increasing the total degradation rate at elevated temperatures [14].

The main goal of the present work is presenting TiO_2 catalysts enhanced by adding silica and Pt particles which may lead to increase the surface area and charge separation. After that, bactericidal experiments of synthesized catalysts were performed. Furthermore, a practical comparison between pure anatase phase of TiO_2 and mixture of crystalline rutile and anatase phases, was carried out by which one can inactive the bacteria using sunlight or UV light.

2. EXPERIMENTAL SECTION

2.1. Preparation of catalysts

All the chemicals were the analytical grade commercially available from Merck Co. and were used as received.

TiO_2 /SiO_2 nanocrystalline powders with a large specific surface area were prepared using sol-gel route. $TiCl_4$ was used as a starting material. A 10% NH_4OH solution was dropped into $TiCl_4$ solution and the white precipitate which obtained at pH=7 was washed with deionized water until complete removing of Cl^- and NH_4^+ ions, and then a certain amount of deionized water was added to form a suspension. 500 mL of the suspension which contains 0.3 mol titanium was divided into 2 parts. Exact amount of concentrate HNO_3 was added into first and second parts ($[H^+]$/ [Ti] = 0.5 and 2) with strong stirring for 24 h at 343 K. Two stable titanium dioxide sols were formed. An appropriate amount of tetraethylorthosilicate (TEOS) was dropped into these sols until TiO_2/SiO_2 = 40/60 (mole/mole) was obtained. The sols were dried at 313 K and calcined at 673 K for 3 h with a heating rate of 3.3 K/min to obtain TiO_2/SiO_2 catalysts.

2.2. Loading of the Pt

Pt-loaded (1%wt) TiO_2/SiO_2 catalysts were prepared as follow: catalyst powders were stirred in a 1% methanol aqueous solution containing appropriate amount of H_2PtCl_6 and irradiated by two 30 W Hg Lamp for 20 h. During the irradiation, H_2PtCl_6 was photoreduced to disperse Pt metal particles over TiO_2 /SiO_2 photocatalysts. After filtering and washing by distilled water, the photocatalysts were dried at 200 ˚C for 2 h to remove the excess methanol adsorbed on the catalysts surface.

2.3. Characterization of catalysts

The photocatalysts were analyzed by X-ray diffraction (XRD) patterns using Cu Kα radiation (λ =0.1542 nm) on a JEOL, JOX-8030 diffraction meter. Diffraction patterns were taken over the 2θ range of 20-80°. The average crystalline sizes of anatase and rutile were determined according to the Scheerer's equation using the full-width at half maximum (FWHM) of the peak presenting the highest intensity and taking into account the instrument broading. The morphology of the particles was observed by scanning electron microscopy (SEM, Philips- XLQ 30). Surface areas of catalysts were calculated using nitrogen absorption data at 298 K and BET analysis with QUANTASORB. UV-Vis diffuse reflectance spectra (DRS) were obtained for the dry-pressed disk samples using a UV-Vis Spectrophotometer (SHIMADZU-2550). FT-IR spectroscopy was performed on a (SHIMADZU 8400S) spectrometer with KBr beam splitter. The

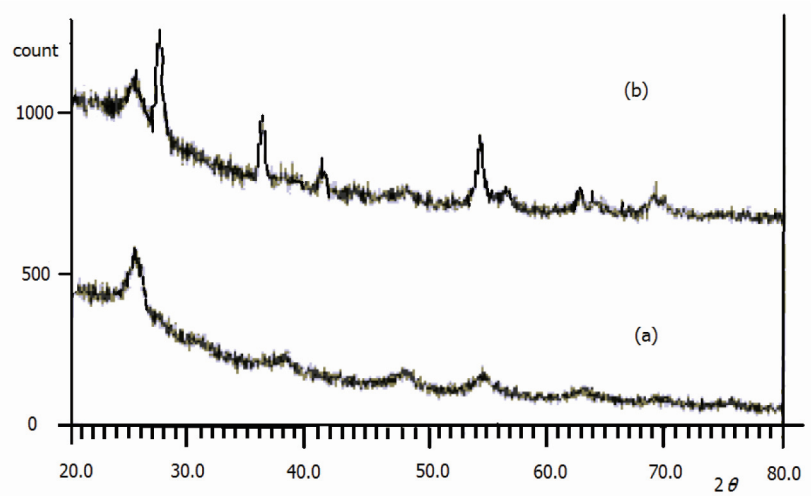

Figure 1: XRD patterns of: (a) pure anatase; (b) mixture of rutile and anatase.

scanning range was from 500 – 4000 cm^{-1} and spectra were collected with a resolution of 2 cm^{-1} by using 20 scans.

2.4. Assessment of antibacterial activities

Escherichia coli (ATTC 0157) **(**Gram (-), rod shape**)** was used as the biological indicator for disinfection efficiency. A microbial suspension of *E. coli* (10^4 CFU/ml) was prepared in 250 mL medium consist of Nutrient Agar (Sigma, St. Louis, USA) was prepared, then was kept in the autoclave at 120 ˚C for 15 min. In separate experiments 5 mL of 0.1 gr/lit of each catalyst suspension was added to 5 mL of microbial medium. Samples were put in the shaker for a few minutes in different conditions include:

1) Under lab condition (25 ˚C, without any direct illumination)

2) Under UV light (250 W, Mercury Lamp)

Photoreactions were carried out for 2 h and samples were taken at intervals. Then samples were cultured at intervals on the NA medium, and were put in the autoclave at 25 ˚C. After 24 h results were collected. The survival rate was obtained by comparing the number of living bacteria on the any examined sample with that of a conventional sample. The survival rate was calculated using eq. (1).

$$S = 100(N_e / N_c) \qquad (1)$$

S: Survival rate in percent

N_e: The number of living bacteria on examination sample

N_C: The number of living bacteria on a conventional sample

3. RESULTS AND DISCUSSION

3.1. Structural analysis of the catalysts

XRD patterns in Fig.1 illustrate the crystalline phases of two samples. As shown, sample 1 ($[H^+]$/ [Ti] =0.5) is pure anatase while sample 2 ($[H^+]$/ [Ti] =2) consists of both anatase and rutile phases. The average crystalline sizes of anatase and rutile in the samples were calculated by applying the Scheerer's formula [15] (eq. 2) on the anatase (101) and rutile (110) diffraction peaks and are shown in Table 1:

$$D = k\lambda / \beta \cos\theta \qquad (2)$$

Where D is the average crystallite size in angstrom, k is a constant which is taken as 0.89 in this work, λ is the wavelength of the X-ray radiation (Cu $k\alpha$

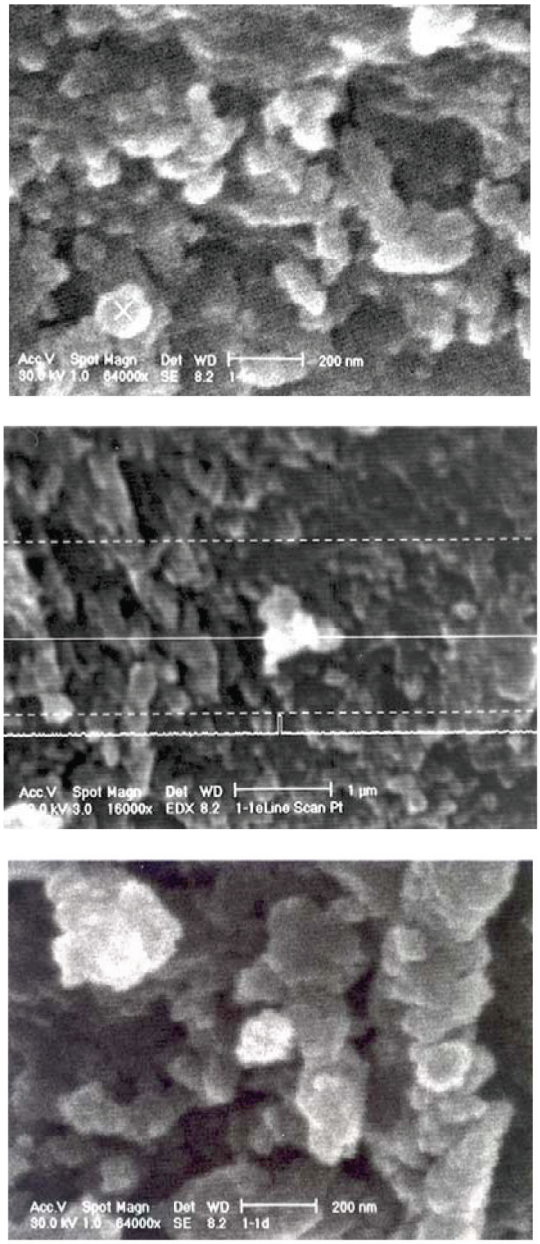

Figure 2: SEM images of pure anatase Pt-TiO_2/SiO_2.

=0.154nm), β is the corrected band broadening (full width at half maximum (FWHM)) and θ is the diffraction angle. The anatase fraction of TiO_2 for the prepared mixed sample was calculated using XRD spectra and eq. 3 [15].

$$f_A = \frac{1}{1+\frac{1}{k}\frac{I_R}{I_A}} \qquad \begin{matrix} k = 0.79 & f_A > 0.2 \\ k = 0.68 & f_A \leq 0.2 \end{matrix} \qquad (3)$$

In this equation f_A is the fraction of anatase phase in the powder, and I_A and I_R are the X-ray intensities of the anatase (101), reflection at $2\theta = 25.3^\circ$ and rutile (110), reflection at $2\theta = 27.4^\circ$ diffraction peaks, respectively. The contents of the anatase phases in the samples were shown in Table 1.

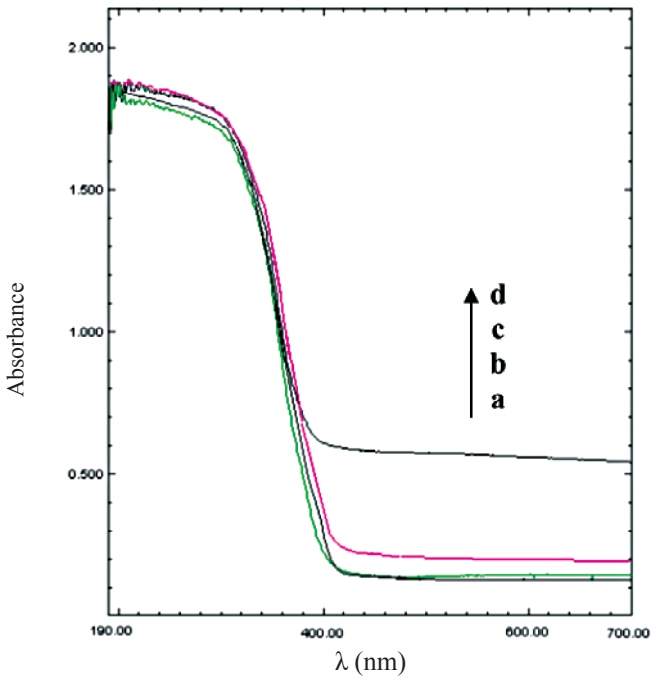

Figure 3: UV-Vis Diffuse Reflectance Spectra of a) TiO_2/SiO_2 (pure anatase), b) TiO_2/SiO_2 (rutile, anatase), c) Pt-TiO_2/SiO_2 (pure anatase) and d) Pt-TiO_2/SiO_2 (rutile, anatase).

As mentioned before, rutile phase was formed by increasing the amount of acid using in the aqueous phase. It should be mentioned that the average size of nanoparticles for the pure anatase catalyst was calculated to be equal 7.7 nm. However, for anatase/rutile mixed catalyst the average particles size is larger than that of the pure anatase. In the mixed catalyst the size of anatase and rutile particles have been calculated to be equal 12.4 and 15.6 nm, respectively. Therefore it is predictable that the specific surface area for the pure anatase catalyst should be larger than that of the mixed catalyst. It is found that the specific surface area is equal to 555 m^2/g for the former and 482 m^2/g for the latter one. It should be mentioned that the surface area of bare titanium dioxide without any support or anchor is not usually as large as these synthesized nanocatalysts. For example surface area of the commercial TiO_2 (P25-Degussa) is about 50 m^2/g [11] and it seems that adding silica has increased the specific surface area of the TiO_2 photocatalysts. Morphological properties of pure anatase Pt-

Table 1: Structural data of synthesized catalysts.

Sample	Particle size[a] (nm)	S_{BET} (m^2/g)	V_p (cm^3/g)	Contents of Anatase[b] (%)	H^+/Ti (mole ratio)
Pure anatase	7	555	0.28	100	0.5
Rutile, Anatase	12.4[c]	482	0.27	39	2
	15.6[d]				

[a]Calculated by eq 1, [b]calculated by eq 2, [c]for anatase, [d]for rutile.

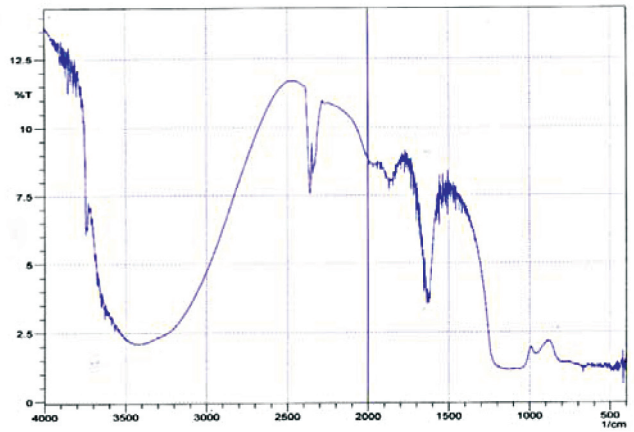

Figure 4: IR spectrum of TiO_2/SiO_2 (pure anatase).

TiO_2 / SiO_2 catalyst were investigated using scanning electron microscopy (SEM). Fig. 2(a-c) shows the SEM micrographs of particles. Fig. 2(a) shows the particles with 16000x magnification. In this image line scanning technique is demonstrated. By using this technique, it was found that doping of Pt particles is not homogenous, for example for the particles shown , Pt content is 17% (wt) while the content of the Pt in average was found to be 1% (wt) using ICP method. Fig. 2(b and c) shows the particles with 64000x magnification. In these figures nanoparticles are clearly observed. As it can be seen, in some parts distinct and round particles are observed and in other parts, the texture of particles is spongy and connected together like a chain.

Fig. 3 shows the UV- Vis DRS of bare and Pt-doped catalysts. As shown, there is no significant difference in the spectra of these catalysts. There is only a narrow distance between the band gap of pure anatase and mixed crystalline photocatalyst. It means that in the case of bigger particle size and existence of rutile phase, a red shift in absorption band, which is not remarkable, is observed [11]. By doping platinum in these photocatalysts again no significant difference is observed in the band gap between the bare and Pt-doped photocatalysts. This means that, the method of deposition of dopant is unable to change the band gap of TiO_2 significantly.

Fig. 4 shows the FT-IR spectra for nanoparticles of bare and pure anatase photocatalyst. The peaks at 940-960 and 1080-1105 cm^{-1}, indicate the vibration bands for Ti-O-Si and Si-O-Si, respectively. The broad absorption peak appearing near 3400 cm^{-1} relates to a stretching vibration of Ti-OH group. At 1620 cm^{-1}, a band assigned to water also appears. These data prove that TiO_2/SiO_2 has been formed. These results are in agreement with those obtained by Hong, Lee and Park [16].

3.2. Antibacterial activities of photocatalysts

Results of antibacterial activities of synthesized catalysts have been shown in Fig. 5 and Fig. 6. The viability of catalysts-treated cells was determined by colony counting after incubation. An *E. coli* suspension without any catalyst was illuminated as a control; also in another experiment, *E. coli* suspension without any catalyst and any illumination was cultured in the lab condition for the control. Fig. 5 shows the survival percentage of bacteria with different catalysts but without any illumination. As shown for the conventional sample, approximately all of the bacteria were alive after 60 min. In this experiment, it can be seen that the pure anatase TiO_2/SiO_2 catalyst is more efficient than the mixed anatase/rutile catalyst. Also the bacterial inactivation is strongly enhanced by doping Pt particles. In this case, 100% destruction is observed after 30 min using pure anatase Pt-TiO_2/SiO_2

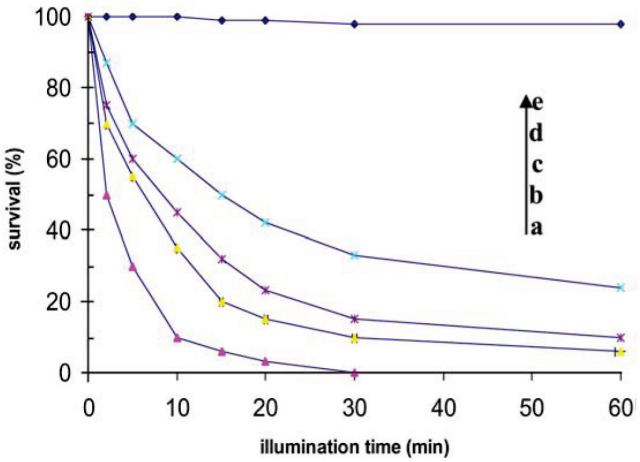

Figure 5: *E. coli* bacteria survival on different catalysts under laboratory light condition: a) Pt - TiO_2/SiO_2 (pure anatase), b) TiO_2/SiO_2 (pure anatase), c) Pt - TiO_2/SiO_2 (rutile, anatase), d) TiO_2/SiO_2 (rutile, anatase) and e) Without catalyst.

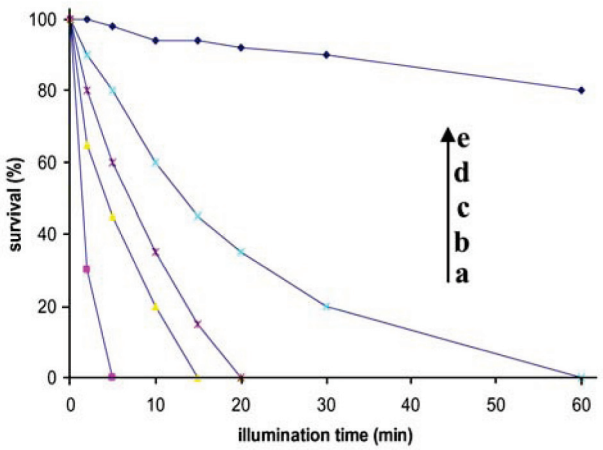

Figure 6: *E. coli* bacteria survival on different catalysts under UV light illumination: a) Pt-TiO_2/SiO_2 (pure anatase), b) TiO_2/SiO_2 (pure anatase), c) Pt - TiO_2/SiO_2 (rutile, anatase), d) TiO_2/SiO_2 (rutile, anatase) and e) without catalyst.

catalyst without any illumination (in the laboratory condition). Different percentages (less than 20%) of survival are observed for other catalysts after 60 min.

Fig. 6 shows photocatalytic activity of different catalysts under illumination of UV light. The bacterial inactivation by UV light strongly is enhanced in the presence of TiO_2 photocatalysts Fig. 6(a-d). In this case the number of active bacteria decreases to a non-detectable value (<1 CFU/ml) after 5 min, when a 250 W mercury lamp is applied in presence of Pt-TiO_2/SiO_2 (pure anatase). This means that 100% destruction of active bacteria has happened by the mentioned photocatalyst and UV

light illumination. Control experiment (Fig. 6e) shows that, more than 80% of *E. coli* survived after 60 min illumination of UV light when photocatalyst is absent. 100% destruction was reached after 15, 20 and 60 min of illumination for the TiO_2/SiO_2 (pure anatase), Pt-TiO_2/SiO_2 (anatase/rutile) and TiO_2/SiO_2 (anatase/rutile) photocatalysts, respectively. Here again the pure anatase catalysts show significant photocatalytic activity with respect to that of the mixed crystalline ones. Larger surface area, finer crystal size and larger amount of anatase phase could be the reasons of better efficiency. Also the effect of doping Pt is remarkable. The presence of Pt increases the effectiveness of the photocatalytic system both in lab condition and under the UV light illumination (Fig. 5 and Fig. 6). The number of active bacteria decreases to a non-detectable value (<1 CFU/ml) only after 5 min., when using Pt-TiO_2/SiO_2 (pure anatase) photocatalyst assisted UV light. In this case the inactivation rate is 3, 4, 12 and 60 times faster than that of TiO_2/SiO_2 (pure anatase), Pt-TiO_2/SiO_2 (anatase/rutile) and TiO_2/SiO_2(anatase/rutile) and in the absent of photocatalyst, respectively.

The beneficial effect of Pt on the photocatalytic disinfection of water is attributed to electron trapping at the semiconductor surface. Pt behaves as an electron scavenger, thus preventing the recombination of electron-hole pairs. The trapping of photoelectrons leaves photogenerated holes available for reaction with the hydroxyl ions present in water to form $OH^{\bullet}$ radicals. This means more $OH^{\bullet}$ radicals would be generated for the bacteria inactivation or the oxidation of organic molecules.

As it is obvious from Fig. 5, the long wavelength behavior could be due to the presence of new electronic states, from the addition of platinum, which lies in the band gap of anatase TiO_2. Thus the surface properties of the catalysts were changed to bring about different photoactivities. But because of lower intensity of illumination (lab condition) the rate of disinfection in this case is much slower than the UV-systems.

4. CONCLUSIONS

TiO_2 sol can be obtained by acid hydrolysis of $TiCl_4$. Different crystalline TiO_2 were obtained using different ratios of H^+/Ti molar equal to 0.5 and 2,. At H^+/Ti =0.5 pure anatase and at H^+/Ti=2 mixture of rutile and anatase were obtained. Significant increment in surface area was obtained by modifying the TiO_2 sols using silica. BET improved the large surface area (550 m^2/g for pure anatase and 482m^2/g for mixture of crystals). In order to increase the photocatalytic activity, Pt particles doped on TiO_2/SiO_2 powders. The bacterial inactivation reactions have been carried out using Pt-TiO_2/SiO_2 (pure anatase), TiO_2/SiO_2 (pure anatase), Pt - TiO_2/ SiO_2 (rutile, anatase) and TiO_2/SiO_2 (rutile, anatase) as catalysts. Antibacterial tests on *E. coli* revealed that the efficiency of the catalysts strongly depends on the crystal of TiO_2. In fact, pure anatase phase is more active in bactericidal effect than that of mixed crystalline one. Also doping Pt has a remarkable effect on both catalysts with substantial difference, and promotes their photocatalytic activities. The addition of Pt (1%) to photocatalytic system decreases the time required for total disinfection (<1 CFU/ml), when photocatalyst concentration is 0.05 g/l.

References

1. J. Ryu, D. S. Park, B. D. Hahn, J. J Choi, W. H. Yoon, K. Y. Kim, H. S. Yun, Applied Catalysis B: Environmental. 83 (2008) 1–7.

2. F. Kskandar, A.B.D. Nandiyanto, K.M. Yun, C.J. Hogan Jr., K. Okuyama, P. Biswas, Adv. Mater. 19 (2007) 1408–1412.

3. F. Sayılkana, M. Asiltürka, N. Kirazb, E. Burunkayab, E. Arpac, H. Sayılkana, Journal of Hazardous Materials. 162 (2009) 1309–1316.

4. T.Y. Leung, C.Y. Chan, C. Hu , J.C. Yu, P.K. Wong, Water Research 42 (2008) 4827–4837.

5. C. Wei, W.Y. Lin, Z. Zainal, N.E. Williams, K. Zhu, A.P. Kruzic, R.L. Smith, K. Rajeshwar, Environ. Sci. Technol. 28 **(***1994) 934.*

6. R.J. Watts, S.H. Kong, M.P. Orr, G.C. Miller, B.E. Henry; Water Res. 29 (1995) 95.

7. H. Sakai, E. Ito, R.X. Cai, T. Yoshioka, Y. Kubota, K. Hashimoto, A. Fujishima; Biochim. Biophys. Acta (BBA)-Gen. Subjects 1201 (1994) 259.

8. W.A. Jacoby, P.C. Maness, E.J. Wolfrum, D.M. Blake, J.A. Fennell, Environ. Sci.Technol. 32 (1998) 2650.

9. T. Matsunaga, R. Tomoda, T. Nakajima, H. Wak, FEM Microbial. Lett. 29 (1985) 211.
10. D.M. Blacke, P.C. Maness, Z. Huang, W.A. Jacoby, E.j. Wolfrum, J. Huang, Separ. Puri Methods. 28 (1999) 1.
11. D. Robert, Y. Bessekhouad, J.V. Weber, N. Chaoui, J. Photochem. Photobio. A: Chem. 167 (2004) 49.
12. V. Brezova, A. Blazkova, L. Karpinsky, J. Groskova, B. Havlinova, V. Jorik, M. Eeppan, J. Photochem. Photobio, A: Chem. 109 (1997) 177.
13. Y.Zhang, G.Xiong, N. Yao, W. Yang, Catalysis Today. 68 (2001) 89-95.
14. T. Sano, N. Negishi, K. Uchino, J. Tanaka, S. Matsuzawa, K. Takeuchi, J. Photochem. Photobio. A: Chem 160 (2003) 93.
15. M. Yan, F. Chen, J. Zhang, M. Anpo, J. Phys. Chem. B, 109 (2005) 8673.
16. S. Hong, M. Lee, S. Park, G. Lee, Catalysis Today, 87 (2003) 99.